Journal of Metals, Materials and Minerals, 33(4), 1752, 2023

Growth of proton conducting strontium cerate composites

C. K. SHILPA[1], S. V. JASIRA[1], V. P. VEENA[1], and K. M. NISSAMUDEEN[1,*]

[1] *School of Pure and Applied Physics, Kannur University, Payyanur Campus, Edat, Kannur, Kerala, 670327, India*

***Corresponding author e-mail:** nisamkm@kannuruniv.ac.in

Received date:
19 May 2023
Revised date
11 August 2023
Accepted date:
1 December 2023

Keywords:
Perovskite;
Proton conduction;
Doped strontium cerates;
Conductivity

Abstract

The increased population and modern way of life have greatly depleted the effectiveness of traditional energy production methods. There is a strong demand for environmentally friendly and renewable alternatives to replace the old systems. Sustainable energy production systems have emerged as a vital replacement for the conventional use of fossil fuels. Among these, solid oxide fuel cells (SOFCs) play a significant role. Recently, researchers have developed electrolyte components for SOFCs using proton-conducting perovskites with excellent conductivity. This critical assessment presents a yearly overview of innovative strategies for utilizing doped strontium cerate perovskites in energy production systems, a novel approach. The importance of identifying dopants that can enhance conductivity and stability in strontium cerate composites is emphasized, creating a crucial element for high-performance energy systems. Through a comparative study, it's been found that rare earth elements with smaller ionic radii, such as thulium-doped strontium cerium zirconate in an additional composite form, can outperform the traditionally used ytterbium-doped strontium cerate composites in proton-conducting applications.

1. Introduction

Over the years people have been utilizing fossil fuels for energy generation. A large fraction of mankind is using these energy sources to upgrade and boost the standards of their life. This conventional source of energy is under exhaustion due to population growth and consumption. To overcome this threat, the researchers have built sustainable, well-structured, labor and time-saving energy systems that could replace fossil fuel combustion. Such inventions are essential and necessary for the future generation. From the critical analysis of researchers, it was found that SOFCs act as an effective alternative to the traditional energy systems. A solid oxide fuel cell is a highly efficient and low-cost electrochemical cell capable of generating energy directly by the oxidation of solid oxide electrolytes. Even though these cells have high theoretical efficiency (approx. 85%), their stationary applications are hindered due to high operating temperatures. So, an appropriate ceramic/ solid oxide material that can be used as an electrolyte in SOFC in the intermediate and low-temperature range has to be addressed.

SOFCs based on most established yttria-stabilized zirconia operate in the high-temperature range (800°C to 1000°C) and require highly expensive materials like fuel cell interconnectors and parts. Also, large start-up times and hefty energy inputs to heat the cell at this operating temperature are required for SOFCs. Thus, SOFCs should be reasonably designed at an intermediate temperature range (400°C to 700°C) to give an efficient power output. During the process of attaining intermediate temperature SOFC, the electrolyte resistance rapidly increases, thus the practical applications are permanently hindered. Therefore, researchers have optimized two approaches to reduce the resistance of electrolytes. The former is to reduce the thickness of the electrolyte and the latter is to find an efficient alternative probe having high ionic conductivity than yttria-stabilized zirconia.

For several years, researchers have focused on oxygen ion conductors as a substitute for yttria-stabilized zirconia. But recently, a fascinating interest has thriven to proton conducting perovskite oxides. Generally, these oxides have characteristic ABO_3 structure, where the alkali earth elements occupy the A site (Ba, Sr, Ca), and tetravalent elements occupy the B site (Ce, Zr). To improve the proton conductivity, the B site of the ABO_3 structure is incorporated with trivalent elements such as Y, Nd, Sm, Yb, In, Eu, Gd, etc. by introducing oxygen vacancies. Strontium cerate perovskites (SCP) show proton conduction when exposed to hydrogen/water vapor atmospheres. The crystal structure of strontium cerate perovskite is represented in Figure 1 [1].

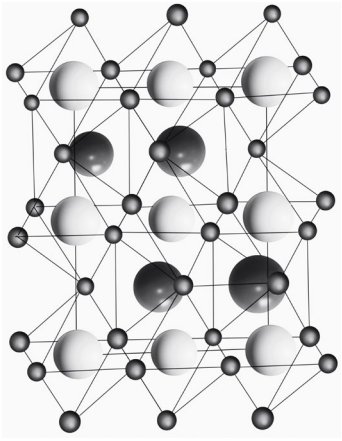

Figure 1. Crystal structure of strontium cerate perovskites with Sr^{2+} (Black big atom), Ce^{4+}(white atom), O^{2-} (small black atom).

For a better understanding of the process, the underlying mechanism behind proton conduction has to be addressed. Proton conduction is a temperature-activated process commonly seen in water-containing atmospheres. Proton conduction occurs due to the inhabitation of proton defects in oxide when the oxides (comprising oxygen vacancies) detach and absorb water from the neighboring wet atmosphere [2].

Protons are allocated in the material through the hydration of oxygen vacancies. These oxygen vacancies are created by doping trivalent elements in the B site of the perovskite. Trivalent elements are used as dopants in solid electrolytes due to their odd number of valence electrons. Owing to this property, vacancies or holes are formed in the crystal structure facilitating the movement of protons. These holes act as charge carriers, allowing the conduction of protons through the material, consequently enhancing its proton conductivity. In solid oxides, the protons get diffused by the Grotthuss mechanism or vehicle mechanism. According to the Grotthuss mechanism, protons reorient in the direction of oxygen nearby and jump to it. Here the oxygen-hydrogen bond has greater importance. The bond strength can be modified by stretching, shortening, and reorienting the atoms around it [3]. Whereas in vehicle mechanism the water molecules cluster with the electrolyte membrane to form a proton conducting channel. Here the water molecule acts as a vehicle to carry protons. Both the mechanisms are emphasized in Figure 2.

Strontium cerate like perovskites such as strontium zirconate, barium cerate, and calcium zirconate were extensively studied in order to find out the proton conduction. These perovskites were doped with trivalent rare earth elements such as ytterbium, yttrium, neodymium, and indium for proton conduction enhancement. Extensive tests on the electrical performance of doped zirconate and cerate proton conductors were studied, out of which zirconate perovskites have low proton conduction of the order of 10^{-3} S·cm^{-1} compared to cerates having that of 10^{-2} S·cm^{-1} to 10^{-1} S·cm^{-1} at 600°C. Application of SCP was hindered due to lower stability and decomposition of cerates into carbonates and hydroxides in the carbon dioxide atmosphere. However, the addition of zirconium ions in the B sites of perovskites has shown high mechanical strength and chemical stability. Thus, the cerate–zirconate combination has been a good candidate for electrolytes in fuel cells. In the present review, we categorize the annual development of SCP and also culminate the best adequate dopants for SCP nano phosphors to achieve high conductivity with satisfactory stability [4]. The annual studies on proton conduction in strontium cerates are represented in Figure 3 using the SCOPUS database with the keyword ‘proton conduction in strontium cerate’

.

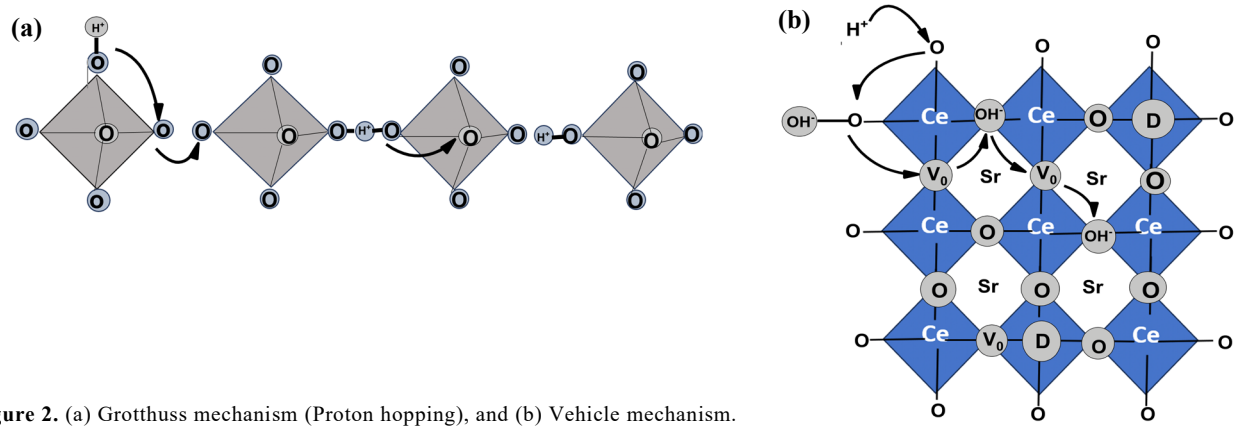

Figure 2. (a) Grotthuss mechanism (Proton hopping), and (b) Vehicle mechanism.

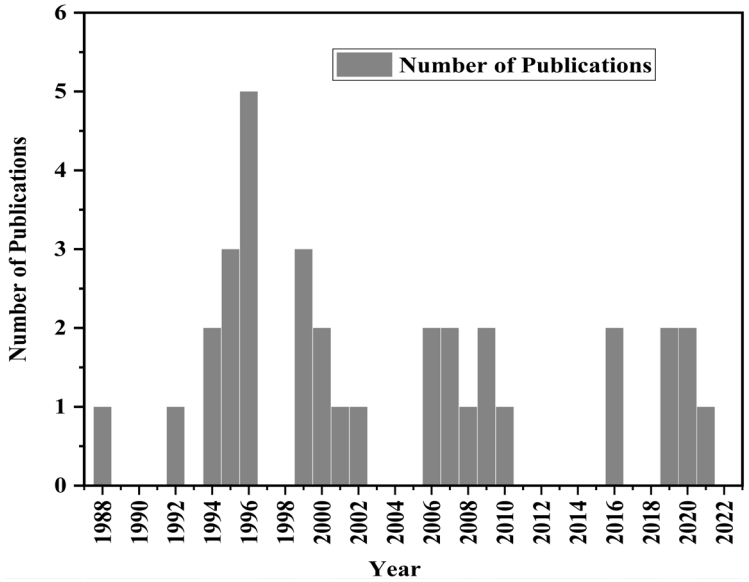

Figure 3. Total number of articles published on ‘proton conduction in strontium cerate’ in the year duration 1988-2023 using the Scopus database.

2. Proton conducting SCP

The introductory work in SCP nano phosphors was done by Iwahara *et al.,* in 1981. In this work, strontium cerate and its derivatives were synthesized through a solid-state reaction in which proton conduction was evaluated by measuring the emf of the gas cell. They assembled a steam concentration cell with a steady stable current in the temperature range 600°C to 800°C using $SrCe_{0.95}Yb_{0.05}O_{3-\alpha}$ and $SrCe_{0.95}Mg_{0.05}O_{3-\alpha}$ as a solid electrolyte to generate hydrogen gas. The team found higher proton conduction in strontium cerate-based sintered oxides in the hydrogen-containing atmosphere at high temperatures. The composition of elements for proton conductivity measurement was optimized by conducting experiments followed by varying the composition of the material to find the best-performing combination. They also generated a hydrogen-oxygen fuel cell using strontium cerate doped with scandium, yttrium, indium, zinc, neodymium, samarium, and dysprosium and it was found that this cell acts as a direct hydrogen gas conversion cell to generate electricity at 700°C, 800°C, and 1000°C. Thus, the steam electrolytic cell performs a reciprocal operation of hydrogen fuel cell [5]. In 1982, they also investigated the application of $SrCe_{0.95}Yb_{0.05}O_{3-\alpha}$, $SrCe_{0.95}Sc_{0.05}O_{3-\alpha}$, $SrCe_{0.95}Y_{0.05}O_{3-\alpha}$ as solid electrolytes in high-temperature hydrogen-oxygen fuel cells and also $SrCe_{0.90}Sc_{0.10}O_{3-\alpha}$ in the steam electrolysis cell. These electrolytes were synthesized in the former way and operated stably in the temperature range 800°C to 1000°C. From a comparative study, it was confirmed that proton conduction is more valuable than oxygen conduction. These cells with proton conductive electrolytes show unique and distinctive advantages like the generation of uncontaminated hydrogen from the electrolysis cell. The privation of fuel circulation due to the absence of water molecules at the fuel cell electrode is also promising. Though the conductivities of these protonic conductors are not sufficiently greater, such electrolytic cells are apt for reciprocal direct energy conversion of hydrogen to electricity and vice-versa, with maximum conversion efficiency [6].

However, the strategic mechanism behind the proton conduction is still vague. So, a new intention to uplift the proton conductivity in doped SCP was performed by Uchida *et al*., in 1983, and were able to give a correlation between proton and hole conductivity by introducing the concept of total conductivity. They suggested that total conductivity can be measured in terms of dopant concentration and partial pressure of water vapor/ oxygen in the gas embedding the specimen ($SrCe_{1-x}Yb_xO_{3-\alpha}$, x=0-0.1). It was found that proton conductivity has a linear relation with dopant concentration and partial pressure of water. Likewise, hole conductivity has a direct relation to the partial pressure of the oxygen. In conclusion, the total conductivity was enhanced when the partial pressure of water was low and oxygen was high, which implies that the proton conduction is due to holes [7].

An indirect proof of proton conduction in terms of solubility was then reported by Ishigaki *et al.,* in 1986. The work mainly focused on computing the concentration of deuterium by dissolving deuterium into $SrCe_{0.95}Yb_{0.05}O_{3-\alpha}$. They have obtained a resultant concentration of 0.01 mol to 0.05 mol deuterium in 1 mol of the perovskite. This large solubility has been attributed to the cause of proton conduction in the perovskite [8].

Utilizing the $SrCe_{0.95}Yb_{0.05}O_{3-\alpha}$ as the diaphragm, a hydrogen extractor was constructed by Iwahara *et al*., in 1987 in order to extract hydrogen at a rate of a few liters per hour from ethane, steam, or pyrolyzed gas of carbon monoxide and water mixture. The ceramic was then exposed to hydrogen gas at the anode and oxygen gas at the cathode (called the ultimate fuel cell condition). Here the electronic conductivity measurement has varied linearly with partial pressure of oxygen, recommending that, the charge carriers were positive holes. They constructed a steam electrolyzer using $SrCe_{0.95}Yb_{0.05}O_{3-\alpha}$ and $SrCe_{0.90}Yb_{0.10}O_{3-\alpha}$ and were able to attain hydrogen production efficiency above 95% in the temperature range 700°C to 900°C. Also, the current density was 0.2 $A{\cdot}cm^{-1}$ at 800°C and hence proved that the steam electrolyzer gave an appreciable performance. They also suggested that this ceramic electrolyte was dense and could be further drawn into thin films in order to reduce the ohmic loss [9].

Later work was conducted by Uchida *et al.,* in 1989 by dissolving water vapor in $SrCe_{0.95}Yb_{0.05}O_{3-\alpha}$ to find the proton concentration in the compound. At variable temperatures and partial pressure, the proton concentrations were evaluated, and obtained the proton concentration of 2 mol% at 600°C and 1.1 mol% at 1000°C. They were also able to account for three simultaneous equilibria between oxide and the atmosphere [10]. The clarification regarding the equilibria of proton generation was then done by the same team and showed that the proton thus formed can reversibly turn to water vapor at high temperatures [11]. The evolved water vapor amount was then calculated and found that the amount was linearly related to dopant concentration with an ultimate absence of water vapor occurrence at 1300°C [12].

Up to that time proton conductivity, proton concentration, and electrolyzer stability were studied. Now work on direct sensing of hydrogen has been found by Yajima *et al.,* in 1990 by utilizing $SrCe_{0.95}Yb_{0.05}O_{3-\alpha}$ with hydrated aluminum phosphate alone and $SrCe_{0.95}Yb_{0.05}O_{3-\alpha}$ with hydrated $AlPO^{4-}(La_{0.6}Sr_{0.4})_{0.99}CoO_{3-\delta}$, as standard material in hydrogen /steam sensor. The later sensor showed an effective fast linear response and stability while compared to $SrCe_{0.95}Yb_{0.05}O_{3-\alpha}$ with hydrated AlPO4 reference alone. The relation between oxygen vacancy α and proton conduction was then studied by varying α from 0 to 0.05 in x% yttrium and y% niobium doped strontium cerate and found a linear response in conductivity with increase in temperature and also estimated that proton conductivity with zirconium incorporated to cerium site $SrCe_{0.95}Y_{0.05}O_{3-\alpha}$ have shown no change in conductivity as α is independent on concentration of zirconium [13]. Even though several studies regarding proton conduction were done, its applicability was restricted due to minimal conductivity. A comparable higher possible conductivity was found to be 10 $S{\cdot}cm^{-1}$ to 2 $S{\cdot}cm^{-1}$ in $SrCe_{0.95}Yb_{0.05}O_{3-\alpha}$ at 1000°C among lanthanum, gadolinium, ytterbium, and yttrium doped in the same concentration.

Soon after this work, Inglian *et al*., in 1994 developed perovskites by doping thulium, samarium, holmium (trivalent), and europium (divalent) on SCP, which gave a promising result. They found that thulium-doped SCP provided three times the conductivity given by Ytterbium doped strontium cerate at 1000°C and seven times the conductivity given by ytterbium doped strontium cerate at 500°C whereas holmium doped strontium cerate showed same conductivity range as ytterbium doped strontium cerate. But the conductivities

of europium and samarium doped strontium cerate were very small. This predicts the fact that smaller ionic radii of rare earth elements could generate larger conductivity. Also, when these rare earth elements were replaced by tetravalent cerium sites, they give rise to an orthorhombic perovskite [14].

In order to prevent the starting material impurities in the solid-state reaction route of $SrCe_{1-x}Yb_xO_{3-\alpha}$ (x=0, 0.025, 0.05), Zheng *et al.,* in 1995 replaced the processing media of alumina balls and crucible with zirconium dioxide balls and crucible. Since the doped strontium zirconate itself is a proton conductor, an increment in conductivity as expected occurred. The conductivity also increased with higher dopant concentration and its variation with temperature was rapidly visible in the air medium [15].

A new effort for the permeation of hydrogen through the proton conductor $SrCe_{0.95}Y_{0.05}O_{3-\alpha}$ was carried out by Guan *et al.,* in 1998 through an impedance, open cell voltage, and gas penetration measurement. The work was carried out in the temperature range 600°C to 800°C using a hydrogen concentration cell and oxygen-hydrogen fuel cell. It was found that a higher proton transference number and lower oxygen ion transference number favored the hydrogen permeation probability [16]. Apart from the solid-state method, liquid-phase methods such as the citrate method and oxalic acid method were first used to prepare $SrCe_{0.95}Tb_{0.05}O_{3-\alpha}$ by Dionysiou *et al*., in 1999. They have found advantages of the citrate method over the oxalic acid method. In the oxalic acid method, they obtain cerium oxide along with $SrCe_{0.95}Tb_{0.05}O_{3-\alpha}$ due to unreacted strontium nitrate in the reaction [17]. Proton conduction in oxide perovskites can be directly evaluated by means of hydrogen permeation across the membrane, Figure 4

Figure 4 illustrates the electrochemical hydrogen extraction from water vapor with thin disc ceramic $SrCeMO_3$ (M: dopant) as a solid electrolyte and platinum electrode material. It is possible to electrolyze water vapor using this solid electrolyte. The proton formation mechanism can be explained through the reaction below. The protons (H^+) in the oxide may be provided from water (H_2O) at the expense of the electron holes (h^+).

$$H_2O + 2h^+ \text{ (oxides)} \rightarrow 2H^+ \text{ (oxides)} + \frac{1}{2} O_2$$

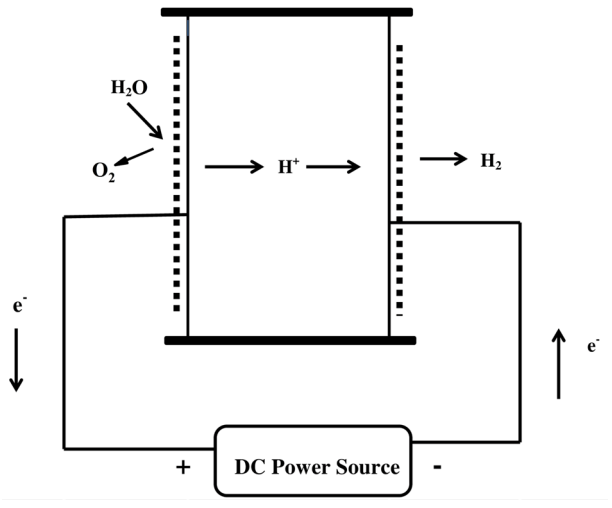

Figure 4. The schematic diagram for electrochemical hydrogen extraction using proton conductor.

A study to implement the existence of oxide ion vacancy was executed by Kek *et al.,* in 2000 by using $SrCe_{0.95}Yb_{0.05}O_{3-\alpha}$ as an electrolyte in nitrogen-hydrogen, nitrogen-oxygen atmosphere. The team found that, in a hydrogen-rich atmosphere, proton conduction is linked to oxide ion conduction. Below 600°C, an immense conductivity of the compound was found in the N_2-5%H_2 atmosphere than in the N_2-O_2 atmosphere, and conductivity in the range 10^{-2} S·cm^{-1} was achieved in both atmospheres at 600°C. But in practical fuel cell applications, restriction due to intermediate conductivity above 900°C was found in the fuel cell environment [18].

Later the application of proton conduction in doped samples of $SrCe_{0.95}Eu_{0.05}O_{3-\alpha}$ and $SrCe_{0.95}Sm_{0.05}O_{3-\alpha}$ in the field of hydrogen permeability was performed by Song *et al.,* in 2004. The well-established setup for measuring hydrogen permeation rates was chosen and $SrCe_{0.95}Eu_{0.05}O_{3-\alpha}$ exhibited higher hydrogen permeability compared to others. They also estimated an inverse variation of hydrogen permeation flux and electronic conductivity with the partial pressure of vapor [19].

Samees *et al.,* in 2004 synthesized $SrCe_{1-x}Y_xO_{3-\alpha}$ (x=0.025, 0.05, 0.075, 0.1, 0.15, 0.20) and resolved the total conductivity to proton, electron, and ion conductivity at 600°C and 800°C as a function of partial pressure of oxygen and at vapor pressures [0.01 atm and 0.001 atm]. The team found that ionic conductivity was maximum with a value of 5 mS·cm^{-1} at $SrCe_{0.9}Y_{0.1}O_{3-\alpha}$ and proton conductivity was raised with high yttrium content. Compared to stoichiometrically doped strontium cerate, the sub-stoichiometric compound exhibited higher electrical conductivity of 7 mS·cm^{-1} [20].

A hydrogen gas sensor was created by Pasierb *et al.,* in 2006. $SrCe_{1-x}Y_xO_{3-\alpha}$ (x=0, 0.01, 0.025, 0.05, 0.1, 0.20) pellets were synthesized by solid-state reaction, followed by calcination at 1175°C for 12 h. These doped strontium cerate pellets were platinum coated on both sides and attached as a whole to alumina tubes. The researchers constructed the sensor in such a way that open cell voltage was expressed in terms of hydrogen gas partial pressure and temperature. It was found that the gas sensor provides a sensor signal with reasonable repeatability, short recovery time, and response below 2 min [21].

The conductivity measurements of $SrCe_{1-x}Eu_xO_{3-\alpha}$ (x=0.1, 0.15, 0.20) in dry and wet pure hydrogen atmospheres were done in a similar way by Oh *et al.,* in 2009 and found that the material exhibited higher total conductivity in both atmospheres [22]. At the same time, a hydrogen permeation membrane preferably leakage-free $SrCe_{0.9}Eu_{0.1}O_{3-\alpha}$/Ni-$SrCeO_3$ was fabricated by Yoon *et al.,* in 2009 and its hydrogen permeation concentration was measured using Q100MS Dycor Quad Link mass spectrometer. The major significance observed was an enhanced ability to achieve 2.2 cm^3·min^{-1} hydrogen permeation flux at a temperature of 900°C under 20 cm^3·min^{-1} feed gas (25% H_2, 3% H_2O, and balanced with Ar). The linear shrinkage rates of pure, Eu^{3+} doped, and NiO doped $SrCeO_3$ was also analyzed, resulting in a larger shrinkage rate for europium doped strontium cerate owing to coax densification [23]. Parallel work was done for the permeability measurement using a hydrogen permeation reactor system in dry and humid hydrogen conditions, reporting the linear dependence of temperature/hydrogen partial pressure on permeability. Permeability in a dry hydrogen atmosphere is more compared to a humid atmosphere, but decreases due to the secondary cerium oxide phase, resulting in a stable permeability measurement in a humid atmosphere. Also, the membrane can achieve a hydrogen flux of 0.6 cm^3·min^{-1}·cm^{-2}.

The hydrogen pervasion flux is limited by electron transport which was in accordance with the decrease in activation energy from 0.97 eV to 0.89 eV with an increase in hydrogen partial pressure [24].

Surface modification and thermal aging effects of $SrCeO_3$-based hydrogen permeable membrane were noticed by Mather *et al.,* in 2010. A layer of Pt catalyst coated over the hydrogen feed exposed side of $SrCe_{0.90}Yb_{0.10}O_{3-\alpha}$, sealed to dual chamber reactor using SiO_2-B_2O_3-BaO-MgO-ZnO sealant was studied over 500°C to 804°C with Ar being the permeable sweep gas. After being exposed to 14 h in 10% H_2-90% N_2 at 804°C, a flux/permeation maximum of 33 nmol·cm^{-2}·s^{-1} was obtained which was far beyond expectation compared to the non-surface modified membrane. The rate of permeation gradually decreased upon exposure to the same condition over a period of 130 h. However, the flux could be reproduced within 6 days by thermal cycling in the 600°C to 804°C range [25]. Even though $SrCeO_3$ has high proton conductivity, it lacks thermal and chemical stability.

The introduction of Zr to $SrCeO_3$ has furnished an optimistic stable proton conductor. An additional partitioning of B site cation to cerium and zirconium can greatly improve the stability of the host lattice. Li *et al.,* in 2011 introduced an additional B site cation to the host lattice NiO-$SrCe_{0.80}Zr_{0.20}O_{3-\alpha}$ with $SrCe_{0.70}Eu_{0.10}Zr_{0.20}O_{3-\alpha}$ perovskite as inner membrane, by colloidal coating. Hydrogen permeation as a function of water, hydrogen feed partial pressure, flow rate, and temperature in different atmospheres was carried out. They found that the high hydrogen partial pressure, had a ¼ proportionality on hydrogen permeation flux whereas activation energy had an inverse proportionality. Also, a maximum hydrogen flux of 0.23 cm^3·cm^{-2}·min^{-1} for 100% H_2 and 0.21 cm^3·cm^{-2}·min^{-1} for 97 vol% H_2/ 3vol% H_2O in feed gas was achieved at 900°C [26].

In 2012, Li *et al.,* came up with the conductivity of $SrCe_{0.40}Zr_{0.40}Yb_{0.20}O_{3-\alpha}$ synthesized by the solid-state route. They used the dc-four probe technique to analyze the conductivity variation in a wet hydrogen atmosphere at high temperatures. The results from the analysis have proven a linear dependence of conductivity on increasing the temperature from 500°C to 1000°C with the highest conductivity of 4.4×10^{-2} S·cm^{-1} at 1000°C. They applied the same perovskite as an electrolyte for hydrogen-oxygen cells and studied the I-V, and I-P characteristics in 600°C to 850°C. The open circuit voltage diminished from 1.164 V to 1.073 V and the ionic transfer number from 0.996 up to 0.946 on increasing the temperature from 600°C to 850°C [27]. Researchers have adopted several techniques for SCP synthesis, out of which solid-state reaction was performed deeply due to its easiness in sample preparation, Figure 5.

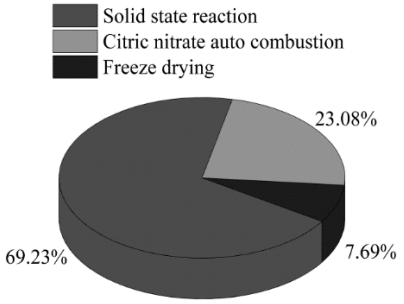

Figure 5. Different synthesis techniques adopted for proton conductivity on an average percentage unit.

Hung *et al.,* in 2015 synthesized $Sr[Ce_{0.6}Zr_{0.4}]_{0.85}Y_{0.15}O_{3-a}$ citrate-EDTA method to find the electrical conductivity and hydrogen permeation flux. Electrical conductivity in various partial pressures of water (2.46×10^{-2} atm and 4.93×10^{-2} atm) and in various atmospheres (hydrogen and air) was estimated using DC-two terminal method and found to exhibit 0.012 S·cm^{-1} conductivity at 900°C. The hydrogen permeation flux depth was measured using a custom-made device in which, a membrane consisting of 10 layers of NiO-$Sr[Ce_{0.6}Zr_{0.4}]_{0.85}Y_{0.15}O_{3-a}$ tape and 1 layer of $Sr[Ce_{0.6}Zr_{0.4}]_{0.85}Y_{0.15}O_{3-a}$ tape, pressed at 90 MPa and sintered at 1450°C for 2 h sealed with Al_2O_3 as the membrane of permeation. When subjected to H_2 atmosphere at one end (NiO-$Sr[Ce_{0.6}Zr_{0.4}]_{0.85}Y_{0.15}O_{3-a}$) and pure Ar at the other ($Sr[Ce_{0.6}Zr_{0.4}]_{0.85}Y_{0.15}O_{3-a}$) from 500°C to 800°C, the hydrogen permeation flux has an increment of 0.084 mmol·min^{-1}·cm^{-2} [28]. Focusing on enhancing the structural and conducting properties, strontium cerium zirconate with varying B site cation concentration and oxygen vacancies got considerable attention. This modified host lattice has been doped with several rare earth elements to study its application.

Doping significantly improved electrical conductivity, lowered synthesis temperature, improved stability, and reduced bandgap. Wang *et al.,* in 2016 doped yttrium to $SrCeO_3$, and formed a composite with ZnO that had potential application in hydrogen permeation membrane. The so-called improved version of the membrane thus, had greater properties such as enhanced electrical conductivities in the hydrogen atmosphere, lower sintering temperature, and greater stability [29]. Doped strontium cerate with additional salt composite could greatly enhance proton conductivity. The choice of salt in the proton conductivity measurement experiment is crucial. Salts selected should have features such as higher proton conductivity, low degradability, chemical stability under operating conditions, high compatibility with composite matrix to ensure homogeneous structure, low cost and high availability for large-scale applications, and minimal environmental impact.

In $SrCeO_3$, protons are transported through the material by hopping among oxygen vacancies. The presence of oxygen vacancies is vital for proton conduction. Doping introduces more oxygen vacancies thus increasing the accessible sites for proton hopping, and enhancing the proton conductivity. Additional salt composites further improve the proton conductivity. The salt composites comprise mobile cations that can move within the ceramic material. The mobile cations (also called proton carriers) facilitate proton conduction by creating protonic channels. As a result, the movement of protons is more efficient in the presence of salt composites. A synergistic effect occurs when $SrCeO_3$ is doped with suitable elements and combined with salt composites. The dopants upsurge the oxygen vacancy number, while the salt composite facilitates the mobile cations that promote the formation of protonic channels. The combination creates an optimal environment for protons to move rapidly through the material, leading to high proton conductivity.

Zhang *et al.,* in 2016 worked on the low-temperature synthesis of novel $SrCe_{0.9}Yb_{0.1}O_{3-a}$ incorporated with (NaCl and KCl), (Li_2CO_3 and K_2CO_3), (NaCl and $CaCl_2$) composite and used as a high-performance electrolyte in intermediate temperature fuel cell. It was observed that in hydrogen atmosphere, these composites showed pure ionic conduction, having maximal conductivities and power densities as (1.2×10^{-1} S·cm^{-1} and 425 mW·cm^{-2}) at 700°C for first composite, (1.0×10^{-1} S·cm^{-1} and 256 mW·cm^{-2}) at 600°C for second composite and (3.3×10^{-2} S·cm^{-1} and 133 mW·cm^{-2}) at 600°C for third composite [30].

Similar to the previous work, a novel set of composite chlorides such as 80 wt% $SrCe_{0.9}Yb_{0.1}O_{3-a}$-20 wt% (Na/K) Cl, 70 wt% $SrCe_{0.9}Yb_{0.1}O_{3-a}$-30 wt% (Na/K) Cl and 80 wt% $SrCe_{0.9}Yb_{0.1}O_{3-a}$-20 wt% ($NaCl/BaCl_2$) were developed by Wang *et al.,* in 2016 at 750°C, quite lower than conventional method. Maximal conductivities and power densities at 700°C were estimated and were found to be (1.2×10^{-1} $S{\cdot}cm^{-1}$ and 471 $mW{\cdot}cm^{-2}$), (3.2×10^{-1} $S{\cdot}cm^{-1}$ and 425 $mW{\cdot}cm^{-2}$) and (9.6×10^{-2} $S{\cdot}cm^{-1}$ and 153 $mW{\cdot}cm^{-2}$) for first, second and third composite respectively [31].

In 2017, Sun *et al.,* synthesized $SrCe_{1-x}Yb_xO_{3-\alpha}$, (x=0, 0.05, 0.1, 0.15)-NaCl/KCl composite electrolytes for intermediate SOFCs at 750°C. It was found that the upper doping limit of Yb^{3+} in $SrCeO_3$ was 15 mol% and no chemical reaction occurred between doped cerate and salt. NaCl/KCl only acted as a binder in the context. Impedance spectroscopy was employed to analyze the electrical conductivity and found that $SrCe_{0.85}Yb_{0.15}O_{3-\alpha}$ -NaCl/KCl composite had a maximal power density of 615 $mW{\cdot}cm^{-2}$ at 700°C [32].

During the same period, $SrCe_{0.85}Er_{0.15}O_{3-\alpha}$ and its composite $SrCe_{0.85}Er_{0.15}O_{3-\alpha}$-NaCl/KCl electrolyte were synthesized by Guan *et al.,* in 2017 using a microemulsion technique and utilized in fuel cells. SCP cubic phase was formed only at higher temperatures above 965°C. At 700°C, the H_2-O_2 fuel cells have achieved a maximal output power density of 304 $mW{\cdot}cm^{-2}$ [33].

Hydrogen production using a steam electrolysis cell was reported by Shi *et al.,* in 2018 and found that $SrCe_{0.9}Y_{0.1}O_{3-\alpha}$ can be used as an electrolyte with excellent cell performance in solid oxide electrolysis cells. The Composite NiO-$SrCe_{0.40}Zr_{0.50}Y_{0.10}O_{3-\alpha}$ highly favored densification of $SrCe_{0.40}Zr_{0.40}Y_{0.20}O_{3-\alpha}$ electrolyte and can be a promising candidate as cathode substances in the solid oxide electrolysis cell. Later, $SrCe_{0.90}Sm_{0.10}O_{3-\alpha}$-NaCl/KCl composite was developed as an electrolyte in SOFCs and studied its performance and conductivity. The conductivity measurement was done using the three-electrode system by the principle of AC impedance spectroscopy in the range 500°C to700°C and in a dry nitrogen atmosphere over a frequency range between 0.1 Hz to 1 MHz. The estimated conductivities were 2.09×10^{-5} $S{\cdot}cm^{-1}$, 1.82×10^{-3} $S{\cdot}cm^{-1}$ and 1.43×10^{-1} $S{\cdot}cm^{-1}$ for SCP, $SrCe_{0.90}Sm_{0.10}O_{3-\alpha}$, $SrCe_{0.90}Sm_{0.10}O_{3-\alpha}$-NaCl/KCl respectively. Here the conductivity of SCP was four orders of magnitude lower than that of the $SrCe_{0.90}Sm_{0.10}O_{3-\alpha}$-NaCl/KCl and $SrCe_{0.90}Sm_{0.10}O_{3-\alpha}$ has conductivity two orders of magnitude lower than that of the composite. A maximum power density of 182 $mW{\cdot}cm^{-2}$ at 700°C in the case of $SrCe_{0.90}Sm_{0.10}O_{3-\alpha}$-NaCl/KCl composite was also noticed [34].

During the same period, $SrCe_{0.9}Yb_{0.1}O_{3-\alpha}$-$(Li/Na)_2CO_3$ and $SrCe_{0.9}Yb_{0.1}O_{3-\alpha}$-LiCl-$SrCl_2$ composite electrolytes were made by Sun *et al.,* in 2018 at 600°C and its performance was studied using H_2-O_2 fuel cells. Conductivities of the above two inorganic salts were investigated by an electrochemical analyzer under a dry N_2 atmosphere in the temperature and frequency range 400°C to 600°C and 1 Hz to 1 MHz respectively. It was found that the conductivities of the former were 0.068 $S{\cdot}cm^{-1}$ to 0.12 $S{\cdot}cm^{-1}$ and the latter was 0.024 $S{\cdot}cm^{-1}$ to 0.035 $S{\cdot}cm^{-1}$ in the range of 500°C to 600°C. The excellent performance of the former composite with 294 $mW{\cdot}cm^{-2}$ power density output equivalent to the current density output 466 $mA{\cdot}cm^{-2}$ was achieved at 600°C [35].

Yadav *et al.,* in 2019 synthesized $SrCe_{0.98}Na_{0.02}O_{3-\alpha}$ by solid state route at 1000°C for 8 h and analyzed its electrical conductivity behavior. It was found that conductivity is closely related to doubly ionized oxygen vacancies [36]. Sol-gel synthesis of $SrCe_{0.6}Zr_{0.3}Er_{0.1}O_{3-\alpha}$-$Na_2CO_3$-$Li_2CO_3$ at 620°C for 1 h was performed by Hu *et al.,* in 2019 and analyzed its conductivity and performance through H_2-O_2 fuel cells in the range 400°C to 600°C. They found that at 600°C the molten salt composite exhibited the highest power density 247.5 $mW{\cdot}cm^{-2}$ and conductivity 1.4×10^{-1} $S{\cdot}cm^{-1}$ [37].

Citric-nitrate auto combustion synthesis of $SrCe_{0.6}Zr_{0.3}Lu_{0.1}O_{3-a}$ followed by reaction with molten salts namely Li_2CO_3 and Na_2CO_3, lead to the formation of $SrCe_{0.6}Zr_{0.3}Lu_{0.1}O_{3-a}$-$Li_2CO_3/Na_2CO_3$ composite electrolyte. The conductivity and performance of the electrolyte were analyzed using a fuel cell by Huang *et al.,* in 2019. The highest conductivity and power densities were 8.6×10^{-2} $S{\cdot}cm^{-1}$ and 255 $mW{\cdot}cm^{-2}$ respectively at 600°C [38].

An involuntary phase separation model by Jia *et al.,* in 2020, with 50% iron incorporated SCP provides the dual phase mixed protonic electronic conductor $SrCe_{0.95}Fe_{0.05}O_{3-a}$ -$SrFe_{0.95}Ce_{0.05}O_{3-a}$ at 1350°C. These oxides are thermodynamically stable and a greater hydrogen permeation flux value 0.38 $mL{\cdot}min^{-1}{\cdot}cm^{-2}$ at 940°C was achieved. Also, they have less degradation in the CO_2 atmosphere, large and stable hydrogen permeation flux of 0.25 $mL{\cdot}in^{-1}{\cdot}cm^{-2}$ at 900°C compared to $SrCe_{0.95}Fe_{0.05}O_{3-a}$ -$SrFe_{0.95}Ce_{0.05}O_{3-a}$ [39]. Soon after, Hu *et al.,* worked on intermediate temperature SOFCs based on citric nitrate auto-combustion synthesis of $SrCe_{0.6}Zr_{0.3}Lu_{0.1}O_{3-a}$ followed by NaCl/KCl and Li_2CO_3/K_2CO_3 addition, for conductivity measurement. It was found that a maximum conductivity of 2.5×10^{-2} $S{\cdot}cm^{-1}$ was achieved at 700°C [40].

Recently Yu *et al.,* in 2021 synthesized $SrCe_{0.90}Yb_{0.10}O_{3-a}$ and analyzed the electrical conductivity in different atmospheres and temperature range 700°C to 900°C. It was noticed that conductivity values decrease in the order of wet hydrogen atmosphere followed by dry hydrogen, dry air, and later in wet air [41]. Up to this time, various doped SCP and its composites have been utilized for proton conductivity measurements as shown in Table 1.

Apart from proton conductivity, strontium cerates and zirconates owe luminescence properties as verified through several articles, Figure 6 [42,43]. So, by combining the two variant behaviors, we can develop a sustainable energy device.

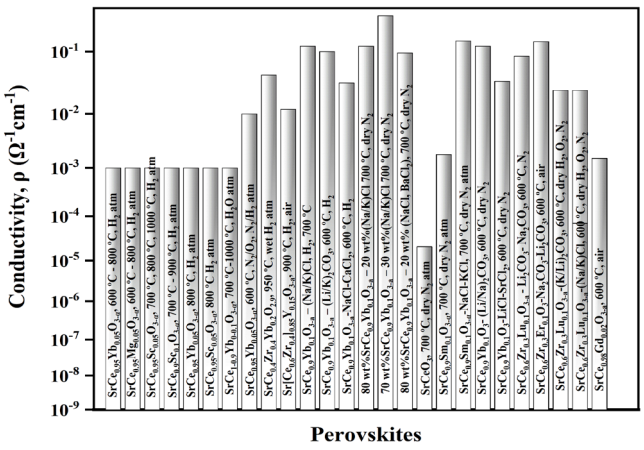

Figure 6. Graphical illustration of the conductivity measurements undergone in SCP

Table 1. Review in a nutshell.

Perovskite	Test conditions	Conductivity, ρ ($\Omega^{-1}\cdot cm^{-1}$)	Year
$SrCe_{0.95}Yb_{0.05}O_{3-\alpha}$	600°C to 800°C, hydrogen atmosphere	10^{-3} to 10^{-2}	1981
$SrCe_{0.95}Mg_{0.05}O_{3-\alpha}$	600°C to 800°C, hydrogen atmosphere	10^{-3} to 10^{-2}	1981
$SrCe_{0.95}Sc_{0.05}O_{3-\alpha}$	700°C, 800°C, 1000ºC, hydrogen atmosphere	10^{-3} to 10^{-2}	1981
$SrCe_{0.90}Sc_{0.1}O_{3-\alpha}$	700°C to 900°C, hydrogen atmosphere or water vapor	10^{-3} to 10^{-2}	1982
$SrCe_{0.95}Yb_{0.05}O_{3-\alpha}$	800°C, hydrogen atmosphere or water vapor	10^{-3} to 10^{-2}	1982
$SrCe_{0.95}Sc_{0.05}O_{3-\alpha}$	800°C, hydrogen atmosphere or water vapor	10^{-3} to 10^{-2}	1982
$SrCe_{1-0.9}Yb_{0-0.1}O_{3-\alpha}$	700°C to 1000°C, water	10^{-3} to 10^{-2}	1983
$SrCe_{0.95}Yb_{0.05}O_{3-\alpha}$	700°C to 800°C, O_2 and D_2O	Conduction predicted	1986
$SrCe_{0.95}Yb_{0.05}O_{3-\alpha}$	600°C to 900°C, hydrogen atmosphere	$\rho_p = 2\rho_e$	1987
$SrCe_{0.95}Yb_{0.05}O_{2.975}$	200°C to 1000°C, N_2/O_2, N_2/H_2	10^{-2} at 600°C	1988
$SrCe_{0.4}Zr_{0.4}Yb_{0.2}O_{2.9}$	500°C to 950°C, wet hydrogen	4.4×10^{-2} at 950°C	2012
$Sr[Ce_{0.6}Zr_{0.4}]_{0.85}Y_{0.15}O_{3-a}$	500°C to 900°C, hydrogen, and air	1.2×10^{-2} at 900°C	2014
$SrCe_{0.9}Yb_{0.1}O_{3-a}$-(Na/K)Cl	400°C to 700°C, hydrogen	1.2×10^{-1} at 700°C	2016
$SrCe_{0.9}Yb_{0.1}O_{3-a}$-$(Li/K)_2CO_3$	400°C to 700°C, hydrogen	1.0×10^{-1} at 600°C	2016
$SrCe_{0.9}Yb_{0.1}O_{3-a}$-$NaCl$-$CaCl_2$	400°C to 700°C, hydrogen	3.3×10^{-2} at 600°C	2016
80 wt% $SrCe_{0.9}Yb_{0.1}O_{3-a}$-20 wt% (Na/K)Cl	500°C to 700°C, dry nitrogen	1.2×10^{-1} at 700°C	2016
70 wt% $SrCe_{0.9}Yb_{0.1}O_{3-a}$-30 wt% (Na/K)Cl	500°C to 700°C, dry nitrogen	3.2×10^{-1} at 700°C	2016
80 wt% $SrCe_{0.9}Yb_{0.1}O_{3-a}$-20 wt% $NaCl/BaCl_2$	500°C to 700°C, dry nitrogen	9.6×10^{-2} at 700°C	2016
$SrCeO_3$	500°C to 700°C, dry nitrogen	2.09×10^{-5} at 700°C	2018
$SrCe0.9Sm_{0.1}O_{3-\alpha}$	500°C to 700°C, dry nitrogen	1.82×10^{-3} at 700°C	2018
$SrCe_{0.9}Sm_{0.1}O_{3-\alpha}$-NaCl-KCl	500°C to 700°C, dry nitrogen	1.43×10^{-1} at 700°C	2018
$SrCe_{0.9}Yb_{0.1}O_{3-\alpha}$-$(Li/Na)_2CO_3$	400°C to 600°C, dry nitrogen	6.8×10^{-2} and 1.2×10^{-1} in 500°C to 600°C	2018
$SrCe_{0.9}Yb_{0.1}O_{3-\alpha}$-$LiCl$-$SrCl_2$	400°C to 600°C, dry nitrogen	2.4×10^{-2} and 3.5×10^{-2} in 500°C to 600°C	2018
$SrCe_{0.6}Zr_{0.3}Lu_{0.1}O_{3-a}$-$Li_2CO_3$-$Na_2CO_3$	25°C to 1000°C, nitrogen	8.6×10^{-2} at 600°C	2019
$SrCe_{0.6}Zr_{0.3}Er_{0.1}O_{3-\alpha}$-$Na_2CO_3$-$Li_2CO_3$	400°C to 600°C, air	1.4×10^{-1} at 600°C	2019
$SrCe_{0.6}Zr_{0.3}Lu_{0.1}O_{3-a}$-$(K/Li)_2CO_3$	400°C to 600°C, dry H_2, O_2, nitrogen.	2.5×10^{-2} at 600°C	2020
$SrCe_{0.6}Zr_{0.3}Lu_{0.1}O_{3-a}$-(Na/K)Cl	400°C to 600°C, dry H_2, O_2, nitrogen	2.5×10^{-2} at 600°C	2020
$SrCe_{0.9}In_{0.1}O_{3-\alpha}$	500°C to 700°C, H_2O D_2O	0.7×10^{-4} at 500°C	2020
$SrCe_{0.98}Gd_{0.02}O_{3-\alpha}$	300°C to 600°C, air	1.54×10^{-3} at 600°C	2021

3. Applications and limitations

SCP functions as a good proton conductor, which makes it a promising host in hydrogen permeation membranes, hydrogen sensors, hydrogen separation from a gas mixture, hydrogen production using steam electrolysis, and oxidative coupling in methane [17]. Even though the proton and oxygen conductivities of SCPs have encountered bulk attention today, there are several shortcomings that hinder their application in technical implementations. In a doped SCP structure, oxygen ion conductivity is minimum up to a threshold of 1173 K. Also, the oxygen ion conduction is large when the size of the unit cell is big. To obtain good proton conductivity, one needs to diminish the unit cell proportions or bring together marked distortions in the perovskite structure to reduce oxygen mobility [42].

Moreover, they are unstable in CO_2 and in the mixtures containing CO_2 and H_2O, forming hydroxides and carbonates. This chemical Instability of doped alkaline earth (strontium, barium) cerates restricts its uses in technical applications. Even though alkaline earth zirconates have better chemical stability in the CO_2 atmosphere, they weakly show proton conduction [43]. A clear-cut substitute of zirconia in the B site of SCP composite exhibits improved proton conduction along with stability, which can be an interesting area of future research.

4. Conclusions and future outlook

The current review mainly focuses on the modification and development of SCP for enhanced performance. From a wide focus on ytterbium-doped SCP, it was seen that conductivity increased with increasing dopant concentration. Also, proton conductivity was directly related to the partial pressure of water vapor in the embedded gas surrounding the specimen ($SrCe_{1-x}Yb_xO_{3-\alpha}$, x=0-0.1). By dissolving deuterium in the same matrix, a correlation between solubility and proton conductivity was established. It was reported that increasing solubility to a large extent resulted in noticeable proton conduction. Not only did the intermolecular features such as solubility, dopant concentration, and partial pressure affect the conductivity, but also a linear response in conductivity with temperature was observed. While considering the ionic radii dependence on conductivity, smaller ionic radii rare earth elements doping could generate larger conductivity. When doped with SCP, europium, and samarium having comparably larger ionic radii resulted in lower conductivity, whereas thulium with the least ionic radii shows higher conductivity. Also, the replacement of alumina balls with zirconia balls during the synthesis could further enhance the proton conductivity. The introduction of Zr to $SrCeO_3$ has furnished an optimistic stable proton conductor. Partitioning of B site cation to cerium and zirconium can greatly improve the stability of the host lattice. Additional composite formation on doped strontium cerate also plays a major role in improving conductivity. The composites exhibit improved microstructural characteristics such as increased grain boundary density, which can facilitate proton migration. From the comparative endeavor through this review, we can conclude that lower ionic radii rare earth such as thulium-doped strontium cerium zirconate with additional composite form can replace the traditionally used ytterbium doped strontium cerate composites for enhanced performance in proton-conducting applications, expecting a wide insight and eventual commercialization in future.

Acknowledgement

The work has no significant financial support that could have influenced its outcome.

Conflict of interest

The authors declare that they have no conflict of interest.

Authors contribution statement

C. K. Shilpa has collected the data, designed the framework, and analyzed the data. C. K. Shilpa, S. V. Jasira, V. P. Veena, and K. M. Nissamudeen carried out the implementation. All the authors have accepted responsibility for the entire content of this manuscript and approved the submission.

References

[1] E. Fabbri, D. Pergolesi, and E. Traversa, "Materials challenges toward proton-conducting oxide fuel cells: A critical review," *Chemical Society Reviews Journal*, vol. 39, pp. 4355-4369, 2010.

[2] F. Lefebvre-Joud, G. Gauthier, and J. Mougin, "Current status of proton-conducting solid oxide fuel cells development," *Journal of Applied Electrochemistry*, vol. 39, pp. 535-543, 2009.

[3] C. Y. Regalado Vera, H. Ding, D. Peterson, W. T. Gibbons, M. Zhou, and D. Ding, "A mini-review on proton conduction of $BaZrO_3$-based perovskite electrolytes," *Journal of Physics: Energy*, vol. 3, pp. 425-435, 2021.

[4] W. Zhang, and Y. H. Hu, "Progress in proton-conducting oxides as electrolytes for low-temperature solid oxide fuel cells: From materials to devices," *Energy Science and Engineering*, vol. 9, pp. 984-1011, 2021.

[5] H. Iwahara, T. Esaka, H. Uchida, and N. Maeda, "Proton conduction in sintered oxides and its application to steam electrolysis for hydrogen production," *Solid State Ionics, vol. 3, pp. 359-363, 1981.*

[6] H. Iwahara, H. Uchida, and N. Maeda, "High temperature fuel and steam electrolysis cells using proton conductive solid electrolytes," *Journal of Power Sources,* vol. 7, pp. 293-301, 1982.

[7] H. Uchida, N. Maeda, and H. Iwahara, "Relation between proton and hole conduction in $SrCeO_3$ -based solid electrolytes under water-containing atmospheres at high temperatures," *Solid State Ionics,* vol. 11, pp. 117-124, 1983.

[8] T. Ishigaki, S. Yamauchi, K. Kishio, K. Fueki, and H. Iwahara, "Dissolution of deuterium into proton conductor $SrFe_{0.95}Yb_{0.05}O_{3-\delta}$," *Solid State Ionics*, vol. 21, pp. 239-241, 1986.

[9] H. Iwahara, H. Uchida, and I. Yamasaki, "High-temperature steam electrolysis using $SrCeO_3$-based proton conductive solid electrolyte," *International journal of hydrogen energy*, vol. 12, pp. 73-77, 1987.

[10] H. Uchida, H. Yoshikawa, and H. Iwahara, "Dissolution of water vapor (or hydrogen) and proton conduction in $SrCeO_3$-based oxides at high temperature," *Solid State Ionics*, vol. 35, pp. 229-234, 1989.

[11] H. Uchida, H. Yoshikawa, and H. Iwahara, "Formation of protons in $SrCeO_3$-based proton conducting oxides. Part I. gas evolution and absorption in doped $SrCeO_3$ at high temperature," *Solid State Ionics*, vol. 34, pp. 103-110, 1989.

[12] H. Uchida, H. Yoshikawa, T. Esaka, S. Ohtsu, and H. Iwahara, "Formation of protons in $SrCeO_3$-based proton conducting oxides. Part II. evaluation of proton concentration and mobility in Yb-doped $SrCeO_3$," *Solid State Ionics*, vol. 36, pp. 89-95, 1989.

[13] T. Yajima, H. Iwahara, H. Uchida, and K. Koide, "Relation between proton conduction and concentration of oxide ion vacancy in SrCeO3 based sintered oxides," *Solid State Ionics,* vol. 40, pp. 914-917, 1990.

[14] W. T. Inglian and L. Z. Hiyi, "Proton conductor of $SrCe_{o.\ gs}L_{no.os}O_x$ (Ln = Eu, Sm, Ho, Tm)," *Journal of materials science letters*, vol. 13, pp. 1032-1034, 1994.

[15] M. Zheng, and B. Zhu, "Proton conductivity in Yb-doped strontium cerates," *Solid State Ionics,* vol. 80, pp. 59-65, 1995.

[16] J. Guan, S. E. Dorris, U. Balachandran, and M. Liu, "Transport properties of SrCeYO and its application for hydrogen separation," *Solid State Ionics*, vol. 110, pp. 303-310, 1998.

[17] D. Dionysiou, X. Qi, Y. S. Lin, G. Meng, and D. Peng, "Preparation and characterization of proton conducting terbium doped strontium cerate membranes." *Journal of Membrane Science*, vol. 154, pp. 143-153, 1999.

[18] D. Kek, N. Bonanos, M. Mogensen, and S. Pejovnik, "Effect of electrode material on the oxidation of H at the 2 metal-SrCeYO interface 0.995 0.95 0.05 2.970," *Solid State Ionics*, vol. 131, pp. 249-259, 2000.

[19] S. J. Song, E. D. Wachsman, J. Rhodes, S. E. Dorris, and U. Balachandran, "Hydrogen permeability of $SrCe_{1-x}M_xO_{3-\delta}$ (x=0.05, M=Eu, Sm)," *Solid State Ion*, vol. 167, pp. 99-105, 2004.

[20] N. Sammes, R. Phillips, and A. Smirnova, "Proton conductivity in stoichiometric and sub-stoichiometric yttrium doped $SrCeO_3$ ceramic electrolytes," *Journal of Power Sources*, vol. 134, pp. 153-159, 2004.

[21] P. Pasierb, A. Biernacka-Such, S. Komornicki, and M. Rękas, "Application of proton-conducting $SrCeO_3$ for construction of potentiometric hydrogen gas sensor," *Optoelectronic and Electronic Sensors*, vol. 6348, pp. 26-30, 2006.

[22] T. keun Oh, H. Yoon, and E. D. Wachsman, "Effect of Eu dopant concentration in $SrCe_{1-x}Eu_xO_{3-\delta}$ on ambipolar conductivity," *Solid State Ion*, vol. 180, pp. 1233-1239, 2009.

[23] H. Yoon, S. J. Song, T. Oh, J. Li, K. L. Duncan, and E. D. Wachsman, "Fabrication of thin-film $SrCe_{0.9}Eu_{0.1}O_{3-\delta}$ hydrogen separation membranes on Ni-$SrCeO_3$ porous tubular supports," *Journal of the American Ceramic Society*, vol. 92, pp. 1849-1852, 2009.

[24] H. Yoon, T. Oh, J. Li, K. L. Duncan, and E. D. Wachsman, "Permeation through $SrCe_{0.9}Eu_{0.1}O_{3-\delta}$Ni–$SrCeO_3$ tubular hydrogen separation membranes," *Journal of the Electrochemical Society*, vol. 156, pp. B791-B794, 2009.

[25] G. C. Mather, D. Poulidi, A. Thursfield, M. J. Pascual, J. R. Jurado, and I. S. Metcalfe, "Hydrogen-permeation characteristics of a $SrCeO_3$-based ceramic separation membrane: Thermal, aging and surface-modification effects," *Solid State Ionics*, vol. 181, pp. 230-235, 2010.

[26] J. Li, H. Yoon, and E. D. Wachsman, "Hydrogen permeation through thin supported $SrCe_{0.7}Zr_{0.2}Eu_{0.1}O_{3-\delta}$ membranes; dependence of flux on defect equilibria and operating conditions," *Journal of Membrane Science*, vol. 381, pp. 126-131, 2011.

[27] J. Li, R. Guo, and H. Jiang, "Preparation and electrochemical properties of $SrCe_{0\cdot4}Zr_{0\cdot4}Yb_{0\cdot2}O_{2\cdot9}$ electrolyte," *Bulletin of Materials Science*, vol. 35, pp. 957-960, 2012.

[28] I-M. Hung, Y-J. Chiang, J. S-C. Jang, J-C. Lin, S-W. Lee, J-K. Chang, and C-S. Hst, "The proton conduction and hydrogen permeation characteristic of $Sr(Ce_{0.6}Zr_{0.4})_{0.85}Y_{0.15}O_{3-\delta}$ ceramic separation membrane," *Journal of the European Ceramic Society*, vol. 35, pp. 163-170, 2015.

29] T. Wang, H. Zhang, B. Meng, X. Wang, J. Sunarso, X. Tan, and S. Liu, "$SrCe_{0.95}Y_{0.05}O_{3-\delta}$-ZnO dual-phase membranes for hydrogen permeation," *RSC Advances*, vol. 6, pp. 36786-36793, 2016.

[30] W. Zhang, M. Yuan, H. Wang, and J. Liu, "High-performance intermediate temperature fuel cells of new $SrCe_{0.9}Yb_{0.1}O_{3-\alpha}$-inorganic salt composite electrolytes," *Journal of Alloys and Compounds*, vol. 677, pp. 38-41, 2016.

[31] H. Wang, and J. Liu, "Low temperature synthesis of novel $SrCe_{0.9}Yb_{0.1}O_{3-\alpha}$-chlorides composite electrolytes for intermediate temperature protonic ceramics fuel cells," *Ceramics International*, vol. 42, pp. 18136-18140, 2016.

[32] L. Sun, H. Miao, and H. Wang, "Novel $SrCe_{1-x}YbxO_{3-\alpha}$-(Na/K)Cl composite electrolytes for intermediate temperature solid oxide fuel cells," *Solid State Ionics*, vol. 311, pp. 41-45, 2017.

[33] Q. Guan, H. Wang, H. Miao, L. Sheng, and H. Li, "Synthesis and conductivity of strontium cerate doped by erbium oxide and its composite electrolyte for intermediate temperature fuel cell," *Ceramics International*, vol. 43, pp. 9317-9321, 2017.

[34] R. Shi, W. Chen, W. Hu, J. Liu, and H. Wang, "$SrCe_{0.9}Sm_{0.1}O_{3-\alpha}$ compounded with NaCl-KCl as a composite electrolyte for intermediate temperature fuel cell," *Materials*, vol. 11, pp. 1583-1594, 2018.

[35] L. Sun, R. Du, H. Wang, and H. Li, "Intermediate temperature electrochemical properties of Yb^{3+} doped $SrCeO_3$- carbonate and chloride composite electrolytes," *International Journal of Electrochemical Science*, vol. 13, pp. 5054-5060, 2018.

[36] D. Yadav, U. Kumar, G. Nirala, and S. Upadhyay, "Electrical conduction and relaxation in perovskite oxide $SrCe_{0.98}Na_{0.02}O_3$ synthesized by solid-state route," *Macromolecular Symposia*, vol. 388, pp. 1900020-1900026, 2019.

[37] W. Hu, W. Chen, and H. Wang, "Synthesis and electrochemical properties of intermediate temperature $SrCe_{0.6}Zr_{0.3}Er_{0.1}O_{3-\alpha}$ -molten carbonate composite electrolyte," *International Journal of Electrochemical Science*, vol. 14, pp. 3229-3235, 2019.

[38] D. Huang, Y. Han, F. Wu, and H. Wang, "Intermediate temperature electrochemical properties of lutetium-doped $SrCeO_3$/$SrZrO_3$-molten carbonate composite electrolyte," *Ceramics International*, vol. 45, pp. 10149-10153, 2019.

[39] L. Jia, S. Ashtiani, F. Liang, G. He, and H. Jiang, "Hydrogen permeation through dual-phase ceramic membrane derived from automatic phase-separation of $SrCe_{0.50}Fe_{0.50}O_{3-\delta}$ precursor," *International Journal of Hydrogen Energy*, vol. 45, pp. 4625-4634, 2020.

[40] W. Hu, W. Chen, and H. Wang, "Electrochemical properties of lutetium and zirconium co-doped $SrCeO_3$ composite electrolyte for intermediate temperature for solid oxide fuel cell," *International Journal of Electrochemical Science*, vol. 15, pp. 3157-3163, 2020.

[41] Q. Yu, Y. Ren, J. Mi, L. Hao, H. Liu, S. Li, S. Li, S. Li, M. Du, and M. Liu, "Microstructure and electrical conductivity of 10% Yb-doped $SrCeO_3$ ceramics," *Progress in Natural Science: Materials International*, vol. 31, pp. 672-678, 2021.

[42] R. L. Cook, and A. F. Sammells, "On the systematic selection of perovskite solid electrolytes for intermediate temperature fuel cells," *Solid State Ionics*, vol. 45, pp. 311-321, 1991.

[43] S. Gopalan, and A. V. Virkar, "Thermodynamic stabilities of $SrCeO_3$ and $BaCeO_3$ using a molten salt method and galvanic cells," *Journal of The Electrochemical Society*, vol. 140, pp. 1060-1065, 1993.